

# ABSOLUTE DIMENSIONS OF THE ECCENTRIC ECLIPSING BINARY V541 CYGNI

GUILLERMO TORRES<sup>1</sup>, CHIMA D. MCGRUDER<sup>1,2</sup>, ROBERT J. SIVERD<sup>3</sup>, JOSEPH E. RODRIGUEZ<sup>1</sup>, JOSHUA PEPPER<sup>4</sup>, DANIEL J. STEVENS<sup>5</sup>, KEIVAN G. STASSUN<sup>6,7</sup>, MICHAEL B. LUND<sup>6</sup>, AND DAVID JAMES<sup>8</sup>

*Accepted for publication in The Astrophysical Journal*

## ABSTRACT

We report new spectroscopic and photometric observations of the main-sequence, detached, eccentric, double-lined eclipsing binary V541 Cyg ( $P = 15.34$  days,  $e = 0.468$ ). Using these observations together with existing measurements we determine the component masses and radii to better than 1% precision:  $M_1 = 2.335^{+0.017}_{-0.013} M_\odot$ ,  $M_2 = 2.260^{+0.016}_{-0.013} M_\odot$ ,  $R_1 = 1.859^{+0.012}_{-0.009} R_\odot$ , and  $R_2 = 1.808^{+0.015}_{-0.013} R_\odot$ . The nearly identical B9.5 stars have estimated temperatures of  $10650 \pm 200$  K and  $10350 \pm 200$  K. A comparison of these properties with current stellar evolution models shows excellent agreement at an age of about 190 Myr and  $[\text{Fe}/\text{H}] \approx -0.18$ . Both components are found to be rotating at the pseudo-synchronous rate. The system displays a slow periastron advance that is dominated by General Relativity (GR), and has previously been claimed to be slower than predicted by theory. Our new measurement,  $\dot{\omega} = 0.859^{+0.042}_{-0.017}$  deg century<sup>-1</sup>, has an 88% contribution from GR and agrees with the expected rate within the uncertainties. We also clarify the use of the gravity darkening coefficients in the light-curve fitting program EBOP, a version of which we use here.

*Subject headings:* binaries: eclipsing — stars: evolution — stars: fundamental parameters — stars: individual (V541 Cyg) — techniques: photometric

## 1. INTRODUCTION

V541 Cyg (also HD 331102, BD+30 3704, TYC 2656-3703-1,  $V = 10.44$ ) is an early type (B9.5+B9.5) detached, eccentric, double-lined eclipsing binary with a relatively long period of 15.33 days (Kulikowski 1948, 1953) and nearly identical components. The first photoelectric light curve was obtained and analyzed by Khaliullin (1985), but the masses could not be determined dynamically because no spectroscopic observations were available at the time. This was remedied by Lacy (1998), who reported radial-velocity measurements for both components and analyzed them in conjunction with the  $V$ -band light curve from Khaliullin (1985) to obtain the absolute masses ( $\approx 2.2 M_\odot$ ) and radii ( $\approx 1.8 R_\odot$ ) with relative errors of about 4% and 2%, respectively.

The system is noteworthy in that it presents a periastron advance that is dominated by the general relativistic effect, estimated to be several times larger than the classical effects due to tidal and rotational distortions. However, there has been some disagreement over the precise rate of apsidal motion, which is fairly slow and difficult to determine, and how closely it conforms

to theoretical expectations. Some authors have obtained good agreement with the predicted motion, while others have measured a rate of precession that is too slow, and argued that V541 Cyg may belong to a small group of binaries including DI Her and AS Cam that display similar discrepancies. Past speculations about possible shortcomings of General Relativity or alternative theories of gravitation that might explain the puzzle (e.g., Guinan & Maloney 1985) have largely fallen out of favor, and at least in the case of DI Her the “anomalous” apsidal motion has now been shown to be caused by the tilted spin axes of the stars relative to the axis of the orbit (Company et al. 1988; Albrecht et al. 2009).

The motivation for this paper is twofold. Firstly, we note that the precision of the mass and radius estimates by Lacy (1998) was limited by the quality and quantity of his spectroscopic observations. In particular, the masses are not quite precise enough for a meaningful comparison with modern stellar evolution models for this important binary system (see, e.g., Torres et al. 2010), a test that was not performed in the original study by that author. To this end we have obtained a much richer set of high-resolution spectra that allows substantial improvement in the absolute dimensions of the two stars. We also bring to bear additional light curves obtained more recently to supplement the only existing set of photometric measurements by Khaliullin (1985). Secondly, we wish to revisit the determination of the apsidal motion and the comparison with internal structure theory by taking advantage of all existing measurements (light curves, radial-velocity measurements, eclipse timings) in a self-consistent way. Previously this has been done using only the measured times of eclipse.

The paper is organized as follows. Section 2 and Section 3 describe our new spectroscopic and photometric observations of V541 Cyg, and the times of minimum light that have the longest time coverage are presented

<sup>1</sup> Harvard-Smithsonian Center for Astrophysics, 60 Garden St., Cambridge, MA 02138, USA; e-mail: gtorres@cfa.harvard.edu

<sup>2</sup> University of Tennessee, Knoxville, 1408 Circle Drive, Knoxville, TN 37996, USA

<sup>3</sup> Las Cumbres Observatory Global Telescope Network, 6740 Cortona Dr., Suite 102, Santa Barbara, CA 93117, USA

<sup>4</sup> Lehigh University, Department of Physics, 413 Deming Lewis Lab, 16 Memorial Drive East Bethlehem, PA 18015, USA

<sup>5</sup> Department of Astronomy, The Ohio State University, Columbus, OH 43210, USA

<sup>6</sup> Department of Physics and Astronomy, Vanderbilt University, 6301 Stevenson Center, Nashville, TN 37235, USA

<sup>7</sup> Department of Physics, Fisk University, 1000 17th Avenue North, Nashville, TN 37208, USA

<sup>8</sup> Astronomy Department, University of Washington, Box 351580, Seattle, WA 98195, USA

in Section 4. Our combined analysis of all the data is described in Section 5, followed by a summary of the inferred physical properties of the components in Section 6. Then in Section 7 we discuss the comparison of the mass, radius, and temperature determinations for V541 Cyg against current models of stellar evolution, and our new measurement of the rate of apsidal motion of the binary is presented in Section 8. We end with a discussion of these results and final remarks in Section 9.

## 2. SPECTROSCOPIC OBSERVATIONS

V541 Cyg was observed spectroscopically at the Harvard-Smithsonian Center for Astrophysics (CfA) with the Digital Speedometer (DS; Latham 1992) on the 1.5m Tillinghast reflector at the Fred L. Whipple Observatory on Mount Hopkins (AZ). This instrument (now decommissioned) was an echelle spectrograph with a resolving power of  $R \approx 35,000$  equipped with a photon-counting intensified Reticon detector limiting the output to a single order 45 Å wide centered on the Mg Ib triplet at 5187 Å. We gathered 72 exposures between 2000 July and 2004 October with signal-to-noise ratios ranging from 20 to 49 per resolution element of  $8.5 \text{ km s}^{-1}$ . One of the observations was obtained during an eclipse and was excluded from further analysis. Reductions were performed with a custom pipeline, and the wavelength calibration was based on exposures of a Thorium-Argon lamp before and after each science exposure. Exposures of the dusk and dawn sky were taken regularly for the purpose of monitoring instrumental drifts. All spectra are clearly double-lined.

Radial velocities (RVs) were determined by cross-correlation using the two-dimensional algorithm TODCOR (Zucker & Mazeh 1994). Templates (one for each component) were taken from a large library of synthetic spectra based on model atmospheres by R. L. Kurucz (see Nordström et al. 1994; Latham et al. 2002), computed for a range of temperatures ( $T_{\text{eff}}$ ), surface gravities ( $\log g$ ), rotational broadenings ( $v \sin i$  when seen in projection), and metallicities ( $[\text{m}/\text{H}]$ ). The optimum templates were selected by cross-correlating each of our 71 spectra against synthetic spectra covering a wide range of parameters, and seeking the best match as measured by the maximum cross-correlation coefficient averaged over all exposures and weighted by the strength of each spectrum (see Torres et al. 2002).

Experience has shown that the narrow wavelength coverage of our spectra introduces strong correlations between  $T_{\text{eff}}$ ,  $\log g$ , and  $[\text{m}/\text{H}]$  such that optimal matches of similar quality can be obtained by slightly increasing or decreasing these three parameters in tandem. We therefore assumed initially that the metallicity is solar, and held  $\log g$  fixed at values near those determined later in our analysis (Section 6). Because the grid spacing of our library in  $\log g$  is 0.5 dex and the actual values ( $\sim 4.25$  for both stars) are intermediate between two grid points, we repeated the determinations using  $\log g$  values of 4.0 and 4.5, and interpolated the results. Similarly, the comparison with stellar evolution models described in Section 7 points to a composition intermediate between  $[\text{m}/\text{H}] = 0.0$  and  $-0.5$ , so we repeated the determinations at the lower metallicity (for each of the two values of  $\log g$ ) and again interpolated. The resulting best-fit temperatures of the slightly larger and more massive pri-

mary component (star 1) and of the secondary (star 2) are 10650 K and 10350 K, respectively, with estimated uncertainties of 200 K. The  $v \sin i$  values are  $15 \pm 1 \text{ km s}^{-1}$  for both stars. Templates near these best-fit values were used to derive the radial velocities. The flux ratio between the secondary and primary as determined with TODCOR is  $\ell_2/\ell_1 = 0.92 \pm 0.02$  at the mean wavelength of our observations, 5187 Å.

Systematic errors in the radial velocities that may result from spectral lines shifting in and out of the narrow spectral window as a function of orbital phase were investigated by means of numerical simulations as described by Torres et al. (1997). Briefly, we generated artificial composite spectra matching each of the real spectra by combining the two templates scaled by the above flux ratio and with the proper relative Doppler shifts as determined from a preliminary spectroscopic orbital solution. We then processed these artificial spectra with TODCOR in the same way as the real spectra, and compared the input and output Doppler shifts. The differences were applied as corrections to the raw velocities measured from the real spectra, and were typically smaller than  $0.5 \text{ km s}^{-1}$ , which is only about 1/3 of our internal errors. The final radial velocities in the heliocentric frame are listed in Table 1 and include these corrections for systematics as well as small run-to-run adjustments to remove instrumental drifts, as described above. Typical uncertainties are about  $1.5 \text{ km s}^{-1}$ .

In addition to our own observations we have made use in our analysis below of the 16 radial-velocity measurements by Lacy (1998), which, although less numerous and of lower precision than our own, were obtained much earlier (1982–1994) and can help to constrain the periastron advance.

## 3. PHOTOMETRIC OBSERVATIONS

The V-band observations of Khaliullin (1985), which we reanalyze here, consist of 531 differential measurements obtained between 1981 May and 1983 July with a 0.5m reflector at the Crimea Observatory of the Sternberg Astronomical Institute. The comparison star was BD+30 3702 (HD 331103) and the check star was BD+31 3728 (HD 331101). The reported internal precision of these measurements is 0.009 mag.

More recent observations of V541 Cyg were obtained between 2007 May and 2014 November in the course of the Kilodegree Extremely Little Telescope transiting planet program (KELT; Pepper et al. 2007). KELT is an all-sky photometric survey to discover transiting planets around bright host stars ( $7 < V < 11$ ). It uses two telescopes: KELT-North located in Sonoita (AZ), and KELT-South at the South African Astronomical Observatory (SAAO). Both telescope systems are based on a Mamiya 645-series wide-angle 42mm lens with an 80mm focal length ( $f/1.9$ ) giving a field of view of  $26^\circ \times 26^\circ$ . The observations of V541 Cyg reported here were gathered at the northern site with a  $4096 \times 4096$  pixel Apogee AP16E CCD camera ( $9 \mu\text{m}$  pixels, corresponding to  $23''$  on the sky) and a 10–20 minute cadence. V541 Cyg is located in KELT-North field 11 ( $\alpha = 19^{\text{h}} 27^{\text{m}} 00^{\text{s}}$ ,  $\delta = 31^\circ 39' 56''$ , J2000). The telescopes are mounted on a Paramount ME German equatorial mount causing images taken East of the meridian to have a  $180^\circ$  rotation compared to the images to the West (Pepper et al. 2007,

TABLE 1  
HELIOCENTRIC RADIAL VELOCITY MEASUREMENTS OF V541 CYG FROM CFA.

| HJD<br>(2,400,000+) | $RV_1$<br>(km s <sup>-1</sup> ) | $\sigma_1$<br>(km s <sup>-1</sup> ) | $(O - C)_1$<br>(km s <sup>-1</sup> ) | $RV_2$<br>(km s <sup>-1</sup> ) | $\sigma_2$<br>(km s <sup>-1</sup> ) | $(O - C)_2$<br>(km s <sup>-1</sup> ) | Orbital<br>phase |
|---------------------|---------------------------------|-------------------------------------|--------------------------------------|---------------------------------|-------------------------------------|--------------------------------------|------------------|
| 51740.7766          | -57.26                          | 1.35                                | -0.27                                | 27.09                           | 1.30                                | -0.59                                | 0.1654           |
| 51743.8481          | -96.49                          | 2.72                                | +2.75                                | 69.96                           | 2.62                                | -1.32                                | 0.3657           |
| 51743.8753          | -98.75                          | 1.62                                | +0.34                                | 69.06                           | 1.56                                | -2.07                                | 0.3675           |
| 51800.7427          | -37.09                          | 1.31                                | -0.95                                | 4.91                            | 1.26                                | -1.26                                | 0.0751           |
| 51802.6632          | -64.62                          | 1.39                                | +1.02                                | 36.69                           | 1.34                                | +0.09                                | 0.2003           |

NOTE. — This table is available in its entirety in machine-readable form.

TABLE 2  
KELT OBSERVATIONS OF V541 CYG  
EAST OF THE MERIDIAN.

| HJD-2,400,000 | $R$ (mag) | $\sigma$ (mag) |
|---------------|-----------|----------------|
| 54257.770944  | 14.941    | 0.016          |
| 54257.775454  | 14.926    | 0.015          |
| 54257.779964  | 14.903    | 0.015          |
| 54257.784484  | 14.934    | 0.015          |
| 54257.788995  | 14.915    | 0.016          |

NOTE. — This table is available in its entirety in machine-readable form.

TABLE 3  
KELT OBSERVATIONS OF V541 CYG  
WEST OF THE MERIDIAN.

| HJD-2,400,000 | $R$ (mag) | $\sigma$ (mag) |
|---------------|-----------|----------------|
| 54250.936923  | 14.615    | 0.013          |
| 54250.942503  | 14.637    | 0.013          |
| 54276.867035  | 14.658    | 0.011          |
| 54362.631612  | 14.637    | 0.011          |
| 54363.630845  | 14.665    | 0.012          |

NOTE. — This table is available in its entirety in machine-readable form.

2012). As the optics for each telescope are not perfectly axisymmetric, the point spread function (PSF) of the same star in the corner of the images is not the same in each orientation. In addition, the PSF full-width-at-half-maximum (FWHM) varies between 3 and 6 pixels depending on where the star is positioned on the CCD. Therefore, the East and West images have been treated as independent time series throughout the reduction and detrending process. Because of the large PSF ( $\sim 1\text{--}2'$  on the sky), light from neighboring stars is likely to affect the photometry and must be taken to account, as described in Section 5. The passband of these observations resembles that of a very broad  $R$ -band filter.

Reductions and detrending were carried out with a dedicated pipeline that produces three types of light curves for each target star in the program: a raw extracted light curve, a “scaled” version that is the raw light curve with a 90-day median smoothing applied, and a detrended version that uses the Trend Filtering Algorithm (TFA; Kovács et al. 2005). For a detailed description of the KELT data acquisition, reduction, and post-processing, see Siverd et al. (2012) and Kuhn et al. (2016). Because the TFA procedures are tuned for the detection of very shallow, transit-like signals characteristic of exoplanets, the results for objects with very deep ( $\sim 0.7$  mag) eclipses such as those in V541 Cyg are less than optimal. Therefore, for the analysis in this paper we have made use of the “scaled” light curves. The time series East of the meridian consists of 3885 measurements with a typical internal photometric precision of 0.017 mag, and the one to the West has 2940 measurements with typical uncertainties of 0.013 mag. These observations are reported in Table 2 and Table 3, respectively.

#### 4. TIMES OF MINIMUM LIGHT

Numerous times of minimum light have been recorded for V541 Cyg and used over the years to improve the ephemeris. The more recent CCD measurements carry essentially all of the weight, and older photographic or

visual timings that have occasionally been included have such large scatter that they are of little use for determining the apsidal motion. Prior to the publication of the photoelectric light curve of Khaliullin (1985) the most complete light curve of V541 Cyg was the one reported by Karpowicz (1961), based on his extensive series of 161 photographic plates collected with a 14 cm astrograph at Ostrowik near Warsaw (Poland) between 1955 and 1959. From these observations Karpowicz reported three average times of minimum light for the primary and three for the secondary, each determined from plates restricted to time spans of no more than two years. Though perhaps better than other photographic estimates, even those timings give very large residuals by modern standards.

However, it is still possible to extract useful information from this material in the form of one average time of primary minimum and one average time of secondary minimum for the entire series. This can be done by using all of Karpowicz’ original photographic measurements together, which allows more complete coverage of the eclipses and therefore a better definition of the minima. The apsidal motion is slow enough that any change in the separation between primary and secondary eclipse over the four-year interval of these observations is small compared to the uncertainties. We proceeded as follows. We phase-folded the 161 brightness measurements with a preliminary ephemeris based on the analysis below, and then fit the primary and secondary eclipses separately using as a template a model light curve from a preliminary solution to the  $V$ -band data of Khaliullin (1985). After applying a vertical offset to the template by eye, we allowed only a horizontal (phase) shift to fit each eclipse (keeping the shape fixed), and finally converted the phase shifts back to time units. We assigned these measurements to a reference epoch closest to the average time of all photographic observations, obtaining Min I =  $2,436,262.3278 \pm 0.0031$  (HJD) and Min II =  $2,436,269.3158 \pm 0.0031$  (HJD). Table 4 lists

TABLE 4  
TIMES OF MINIMUM FOR V541 CYG.

| HJD<br>(2,400,000+)      | $\sigma$<br>(days) | Type | ( $O - C$ )<br>(days) | Year      | Source |
|--------------------------|--------------------|------|-----------------------|-----------|--------|
| 36262.3278               | 0.0031             | 1    | -0.00007              | 1958.1583 | 1      |
| 36269.3158               | 0.0031             | 2    | +0.00151              | 1958.1775 | 1      |
| 44882.2148 <sup>a</sup>  | 0.0007             | 1    | -0.00026              | 1981.7583 | 2      |
| 44889.2196 <sup>a</sup>  | 0.0005             | 2    | -0.00006              | 1981.7775 | 2      |
| 46998.8424               | 0.0010             | 1    | +0.00024              | 1987.5533 | 3      |
| 48616.3400 <sup>b</sup>  | ...                | 2    | +0.00823              | 1991.9818 | 4      |
| 48839.3870               | 0.003              | 1    | -0.00046              | 1992.5924 | 5      |
| 49168.4947               | 0.0007             | 2    | -0.00183              | 1993.4935 | 6      |
| 49168.4955               | 0.0009             | 2    | -0.00103              | 1993.4935 | 6      |
| 49560.2668               | 0.0008             | 1    | -0.00091              | 1994.5661 | 7      |
| 49889.3770               | 0.001              | 2    | -0.00130              | 1995.4672 | 8      |
| 49904.7145               | 0.00012            | 2    | -0.00171              | 1995.5091 | 9      |
| 49935.3911               | 0.0006             | 2    | -0.00093              | 1995.5931 | 10     |
| 49935.3974 <sup>b</sup>  | 0.0012             | 2    | +0.00537              | 1995.5931 | 11     |
| 50296.4906               | 0.0018             | 1    | +0.00477              | 1996.5818 | 12     |
| 51070.3967               | ...                | 2    | -0.00066              | 1998.7006 | 13     |
| 51109.3918               | ...                | 1    | -0.00154              | 1998.8074 | 13     |
| 51385.4740               | 0.0007             | 1    | -0.00113              | 1999.5632 | 14     |
| 52926.28338              | 0.0001             | 2    | -0.00108              | 2003.7817 | 15     |
| 53524.46196              | 0.0001             | 2    | -0.00099              | 2005.4195 | 15     |
| 53578.7911               | 0.0001             | 1    | -0.00052              | 2005.5682 | 16     |
| 53846.55486 <sup>b</sup> | 0.0007             | 2    | -0.00420              | 2006.3013 | 15     |
| 54659.46742              | 0.0002             | 2    | -0.00086              | 2008.5269 | 17     |
| 54659.46762              | 0.0002             | 2    | -0.00066              | 2008.5269 | 17     |
| 54659.46809              | 0.0001             | 2    | -0.00019              | 2008.5269 | 15     |
| 54782.1712               | 0.0003             | 2    | -0.00036              | 2008.8629 | 15     |
| 55066.5740               | 0.0024             | 1    | +0.00827              | 2009.6415 | 18     |
| 55741.42898              | 0.0007             | 1    | -0.00336              | 2011.4892 | 19     |
| 55741.4299               | 0.0064             | 1    | -0.00244              | 2011.4892 | 20     |
| 55741.43011              | 0.0010             | 1    | -0.00223              | 2011.4892 | 19     |
| 55794.4734               | 0.0017             | 2    | -0.00022              | 2011.6344 | 21     |
| 56876.4377               | 0.0026             | 1    | +0.00242              | 2014.5967 | 22     |
| 56929.4809               | 0.0020             | 2    | +0.00195              | 2014.7419 | 23     |
| 57198.5271               | 0.0026             | 1    | -0.00361              | 2015.4785 | 24     |

NOTE. — Measurement errors ( $\sigma$ ) are listed as published. “Type” is 1 for a primary eclipse, 2 for a secondary eclipse. Uncertainties for the timings with no published errors are assumed to be 0.001 days.  $O - C$  residuals are computed from the combined fit described in Section 5. Sources for the times of minimum light are: (1) Measurement made in this paper (see text) based on the photographic light curve of Karpowicz (1961); (2) Volkov & Khaliullin (1999); (3) Lines et al. (1989); (4) Diethelm (1999a); (5) Diethelm (1992b); (6) Agerer (1994); (7) Sandberg Lacy et al. (1995); (8) Wolf (1995); (9) Guinan et al. (1996); (10) Lacy et al. (1998); (11) Diethelm (1995); (12) Diethelm (1996); (13) Volkov & Khaliullin (1999); (14) Diethelm (1999); (15) Wolf et al. (2010); (16) Smith & Caton (2007); (17) Brát et al. (2008); (18) Hübscher et al. (2010); (19) Hoňková et al. (2013); (20) Hübscher et al. (2012); (21) Hübscher & Lehmann (2012); (22) Hübscher & Lehmann (2015); (23) Hübscher (2015); (24) Hübscher (2016).

<sup>a</sup> Timing from Khaliullin (1985) revised by Volkov & Khaliullin (1999) and ignored in the fit of Section 5 because the same information is already contained in the original light curve used in the global fit.

<sup>b</sup> Measurement not used in the global fit for showing a very large residual ( $> 4\sigma$ ).

these two timings along with all other published photoelectric/CCD timings. We note that, although the table also lists the two timings reported by Khaliullin (1985), we do not use them here because our analysis incorporates the full  $V$ -band light curve from this author, which contains the same information.

In general one expects the times of secondary minimum to be more precisely determined than those of primary minimum for V541 Cyg, on account of the much shorter duration of the secondary eclipse (6 hours) compared to

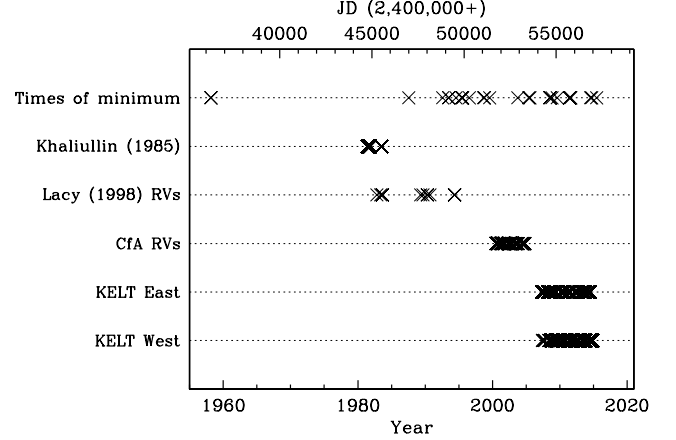


FIG. 1.— Time history of the photometric and spectroscopic observations of V541 Cyg used in this paper.

the primary (16 hours) caused by the large eccentricity and orientation of the orbit. However, this does not seem to be reflected in the formal uncertainties shown in Table 4, possibly due to the heterogeneous nature of these measurements. Many studies have shown that formal timing errors tend to be underestimated, and our analysis below supports this.

## 5. ANALYSIS

The various data sets available for V541 Cyg are complementary in many ways. For example, the light curve of Khaliullin (1985) is of high quality but has incomplete coverage of the primary eclipse. The KELT data, on the other hand, have somewhat lower precision but offer essentially complete coverage of all phases, aiding in determining some of the geometric properties of the orbit. These two photometric time series provide strong constraints on the location of the line of apsides at two epochs some three decades apart. The times of minimum light from the previous section provide additional constraints on the apsidal motion over a longer time span of 57 years (see Figure 1). Finally the radial velocities yield constraints of a different nature at other times, particularly on the eccentricity of the orbit, so that the optimum approach is to combine all of these data in a global fit to solve for all orbital parameters simultaneously, including the apsidal motion.

For the analysis of the light curves of this well-detached system we have adopted the Nelson-Davis-Etzel model (Popper & Etzel 1981; Etzel 1981), implemented originally in the widely used EBOP code. The particular version of the light-curve generator in EBOP used here is a rewrite due to Irwin et al. (2011) that also handles apsidal motion<sup>9</sup>, and is especially useful within the framework of the Markov Chain Monte Carlo methodology we apply here. The parameters solved for include the sidereal period  $P_{\text{sid}}$ , a reference time of primary eclipse  $T_0$  chosen to be near the mean of all our times of observation to minimize correlations, the sum of the relative radii  $r_1 + r_2$  normalized to the semimajor axis, the radius ratio  $k \equiv r_2/r_1$ , the cosine of the inclination angle  $\cos i$ , the eccentricity parameters  $\sqrt{e} \cos \omega$  and  $\sqrt{e} \sin \omega$  at  $T_0$ , the rate of apsidal motion  $\dot{\omega}$ , the central surface brightness ratio  $J \equiv J_2/J_1$ , the fraction of third light divided

<sup>9</sup> <https://github.com/mdwarfgeek/eb>.

by the total light ( $L_3$ ), and a magnitude zero point  $m_0$ . Light travel time across the system was accounted for, although the effect is hardly noticeable.

For the limb darkening effect we adopted the linear law with a coefficient  $u$  (assumed to be the same for the two nearly identical components), as experiments with higher-order prescriptions indicated no improvement. The gravity darkening input required by the code is the product of two values: the exponent  $\beta$  of the law relating the emergent bolometric flux to the local surface gravity, and a separate wavelength-specific gravity darkening coefficient,  $y_\lambda$ .<sup>10</sup> Here we assume  $\beta = 1$ , as appropriate for radiative stars, and the coefficients  $y_\lambda$  were set for each passband to values appropriate for the stellar temperatures: 0.67 and 0.68 for the primary and secondary in  $V$ , and 0.59 and 0.61 for the KELT passband. Separate values of the wavelength-dependent parameters  $J$  and  $u$  were considered for the Khaliullin (1985) data and for the two KELT light curves, and magnitude zero points were solved independently for each of the three light curves. Inclusion of the third light parameter was motivated in part by the report of the presence of a close visual companion to V541 Cyg in the *Tycho* Double Star Catalogue (Fabricius et al. 2002), at an angular separation of  $0''.75$  in position angle  $6^\circ 2$  and with a reported brightness difference of about 1.2 mag in the  $V_T$  passband. We note, however, that subsequent observations by Mason et al. (2009) using speckle interferometry did not detect this companion, even though they were sensitive to it. One value of  $L_3$  was included for the  $V$ -band data, and two additional values were used for the KELT data sets because their much larger PSF ( $\sim 1\text{--}2'$ ; Section 3) is different for the east and west (see Section 3).

For the radial velocities we assumed pure Keplerian or-

bital motion, and solved for the velocity semi-amplitudes  $K_1$  and  $K_2$ , the center-of-mass velocity  $\gamma$ , as well as for a possible offset  $\Delta$  between the velocity zero points for the primary and secondary. The latter may arise, for example, from template mismatch in the cross-correlation procedure. The parameters  $\gamma$  and  $\Delta$  were solved independently for our own RVs and those of Lacy (1998).

The times of minimum light were incorporated using the formalism of Lacy (1992) for the ephemeris curve solution. We note that the EBOP light-curve generator used here assumes  $T_0$  is a time of inferior conjunction, rather than a time of minimum light, but the difference for this system is negligible.

Our method of solution used the `emcee`<sup>11</sup> code of Foreman-Mackey et al. (2013), which is a Python implementation of the affine-invariant Markov Chain Monte Carlo ensemble sampler proposed by Goodman & Weare (2010). Uniform priors over suitable ranges were used for most parameters, and modified Jeffreys priors were used for third light and the jitter parameters (Gregory 2005), although the results are insensitive to these assumptions. Relative weighting between the different data sets was handled by including additional adjustable parameters to inflate the observational errors, which were solved for self-consistently and simultaneously with the other parameters (see Gregory 2005). To inflate the uncertainties of the three light curves we adopted simple scale factors  $f(V)$ ,  $f(\text{KELT east})$ , and  $f(\text{KELT west})$ , as is customary, and for the radial velocities and the times of minimum we used separate “jitter” terms for the primary and secondary ( $\epsilon_{\text{RV},1}$ ,  $\epsilon_{\text{RV},2}$ ,  $\epsilon_{\text{Min I}}$ ,  $\epsilon_{\text{Min II}}$ ) that we added quadratically to the published uncertainties. For the RVs of Lacy (1998), which have no published uncertainties, we assumed errors of  $2.5 \text{ km s}^{-1}$ . The RV jitter terms were independent for the CfA velocities and those of Lacy (1998).

Initial solutions converged to a value of the radius ratio  $k$  larger than unity, which for main-sequence stars such as those in V541 Cyg is inconsistent with a derived mass ratio that is smaller than unity. This is a common problem in fitting light curves of similar stars with partial eclipses, and is due to strong correlations among several of the parameters. In this case, external information must be used to lift the degeneracies, such as a light ratio from spectroscopy (see, e.g., Andersen et al. 1991), which is very sensitive to the radius ratio:  $\ell_2/\ell_1 \propto k^2$ . We therefore imposed a Gaussian prior on the  $V$ -band light ratio generated at each step in our Monte Carlo solution, set by the spectroscopic determination from Section 2,  $\ell_2/\ell_1 = 0.92 \pm 0.02$ . While this measurement is not strictly in the  $V$  passband, the difference is negligible for our purposes because of the similarity in temperature between the components.

The results of our global fit are presented in Table 5, where we list for each parameter the mode of the posterior distributions along with the 68.3% credible intervals. Additional properties derived from the fitted quantities were computed by combining the corresponding Markov chains, link by link, and are reported as well. As anticipated, third light is highly significant for both of the KELT light curves, indicating an appreciable amount of

<sup>10</sup> There has been some confusion in the literature regarding the nature of the input values for gravity darkening expected by the EBOP program in its various implementations, beginning with the original version (Popper & Etzel 1981; Etzel 1981) and continuing with its descendants such as JKTEBOP (Southworth 2013) and the code used here (Irwin et al. 2011). While other light-curve fitting programs deal internally with the wavelength dependence of the flux  $F$  as affected by local gravity  $g$  using either the blackbody formula or model atmospheres, and therefore expect the input values for gravity darkening to be the exponent ( $\beta$  in recent usage) of the bolometric law  $F \propto g^\beta$  for each star (von Zeipel 1924; Lucy 1967; Claret 1998), EBOP has no knowledge of the passband of the observations, or in fact of the absolute temperatures of the stars (by design). Therefore, it is up to the user to supply values appropriate for the wavelength  $\lambda$  and stellar temperatures, as is the case for the limb-darkening coefficients. EBOP adopts a simple Taylor expansion of the wavelength-dependent flux as a function of local gravity of the form  $F_\lambda = F_{0,\lambda} [1 + y_\lambda \beta (g - g_0)/g_0]$  (see, e.g., Kopal 1959; Binnendijk 1960; Martynov 1973; Kitamura & Nakamura 1983), retaining only the linear term consistent with the level of other approximations and the intended application of the model to simple, well-detached binary systems. The input required by EBOP is the product of  $\beta$  and the gravity darkening coefficient  $y_\lambda$ , which depends on wavelength and also temperature. Expressions to compute  $y_\lambda$  are provided in the above references using a blackbody approximation, which is sufficient for our purposes given that the gravity darkening effect is essentially negligible for nearly spherical stars such as those in V541 Cyg. Note that  $y$  is unity for the total (bolometric) flux, but varies significantly as a function of  $T_{\text{eff}}$  and  $\lambda$  and can be larger or smaller than unity. Although the prescription for gravity darkening in terms of the coefficient  $y$  is described in the original documentation for EBOP (Etzel 1980), where the implicit assumption is also made that  $\beta$  is always unity, that document is unpublished and has generally been difficult to obtain, which may have contributed to the confusion.

<sup>11</sup> <http://dan.iel.fm/emcee>.

TABLE 5  
GLOBAL SOLUTION FOR V541 CYG.

| Parameter   | Value                                     |
|---|---|
| $P_{\text{sid}}$ (days) .....                               | $15.33789922^{+0.00000057}_{-0.00000035}$ |
| $T_0$ (HJD-2,400,000) .....                                 | $54621.76727^{+0.00048}_{-0.00053}$       |
| $J(V)$ .....  | $0.9973^{+0.0063}_{-0.0044}$              |
| $J(\text{KELT})$ .....                                      | $0.9984^{+0.0097}_{-0.0070}$              |
| $r_1 + r_2$ .....   | $0.08494^{+0.00042}_{-0.00042}$           |
| $k \equiv r_2/r_1$ .....                                    | $0.9735^{+0.0073}_{-0.0096}$              |
| $\cos i$ .....  | $0.00294^{+0.00034}_{-0.00056}$           |
| $\sqrt{e} \cos \omega_0$ .....                              | $-0.08543^{+0.00021}_{-0.00021}$          |
| $\sqrt{e} \sin \omega_0$ .....                              | $-0.6790^{+0.0011}_{-0.0010}$             |
| $\dot{\omega}$ (deg century $^{-1}$ ) .....                 | $0.859^{+0.042}_{-0.017}$                 |
| $m_0(V)$ .....  | $0.7978^{+0.0016}_{-0.0015}$              |
| $m_0(\text{KELT east})$ .....                               | $14.91747^{+0.00042}_{-0.00036}$          |
| $m_0(\text{KELT west})$ .....                               | $14.63733^{+0.00024}_{-0.00037}$          |
| $L_3(V)$ .....  | $0.0016^{+0.0082}_{-0.0016}$              |
| $L_3(\text{KELT east})$ .....                               | $0.1758^{+0.0096}_{-0.0090}$              |
| $L_3(\text{KELT west})$ .....                               | $0.1161^{+0.0071}_{-0.0104}$              |
| $u(V)$ .....  | $0.339^{+0.063}_{-0.032}$                 |
| $u(\text{KELT})$ .....                                      | $0.408^{+0.077}_{-0.153}$                 |
| $f(V)$ .....  | $1.684^{+0.050}_{-0.055}$                 |
| $f(\text{KELT east})$ .....                                 | $1.544^{+0.016}_{-0.020}$                 |
| $f(\text{KELT west})$ .....                                 | $1.392^{+0.016}_{-0.021}$                 |
| $\epsilon_{\text{Min I}}$ (days) .....                      | $0.0019^{+0.0011}_{-0.0005}$              |
| $\epsilon_{\text{Min II}}$ (days) .....                     | $0.00054^{+0.00033}_{-0.00008}$           |
| $\gamma_{\text{CfA}}$ (km s $^{-1}$ ) .....                 | $-15.48^{+0.22}_{-0.13}$                  |
| $\gamma_{\text{Lacy}}$ (km s $^{-1}$ ) .....                | $-14.68^{+0.65}_{-1.04}$                  |
| $\Delta_{\text{CfA}}$ (km s $^{-1}$ ) .....                 | $-0.30^{+0.26}_{-0.24}$                   |
| $\Delta_{\text{Lacy}}$ (km s $^{-1}$ ) .....                | $+0.3^{+1.5}_{-1.3}$                      |
| $K_1$ (km s $^{-1}$ ) .....                                 | $79.36^{+0.17}_{-0.27}$                   |
| $K_2$ (km s $^{-1}$ ) .....                                 | $81.97^{+0.20}_{-0.24}$                   |
| $\epsilon_{\text{RV},1}(\text{CfA})$ (km s $^{-1}$ ) .....  | $0.06^{+0.40}_{-0.02}$                    |
| $\epsilon_{\text{RV},2}(\text{CfA})$ (km s $^{-1}$ ) .....  | $0.10^{+0.71}_{-0.10}$                    |
| $\epsilon_{\text{RV},1}(\text{Lacy})$ (km s $^{-1}$ ) ..... | $2.5^{+1.0}_{-1.5}$                       |
| $\epsilon_{\text{RV},2}(\text{Lacy})$ (km s $^{-1}$ ) ..... | $3.1^{+1.3}_{-0.7}$                       |
| Derived quantities  |   |
| $P_{\text{anom}}$ (days) .....                              | $15.33790024^{+0.00000056}_{-0.00000034}$ |
| $e$ .....   | $0.4684^{+0.0013}_{-0.0015}$              |
| $\omega_0$ (deg) .....                                      | $262.829^{+0.027}_{-0.030}$               |
| $\dot{\omega}$ (10 $^{-7}$ rad day $^{-1}$ ) .....          | $4.11^{+0.20}_{-0.08}$                    |
| $U$ (years) .....   | $41800^{+1000}_{-1800}$                   |
| $i$ (deg) .....   | $89.832^{+0.032}_{-0.019}$                |
| $r_1$ .....   | $0.04306^{+0.00024}_{-0.00023}$           |
| $r_2$ .....   | $0.04188^{+0.00030}_{-0.00030}$           |
| $q \equiv M_2/M_1$ .....                                    | $0.9681^{+0.0036}_{-0.0040}$              |
| $a$ ( $R_{\odot}$ ) .....                                   | $43.198^{+0.093}_{-0.086}$                |
| $\ell_2/\ell_1(V)$ .....                                    | $0.942^{+0.016}_{-0.013}$                 |
| $\ell_2/\ell_1(\text{KELT})$ .....                          | $0.944^{+0.017}_{-0.015}$                 |
| Phase of Min II at $T_0$ .....                              | $0.457997^{+0.000041}_{-0.000032}$        |

flux is coming from nearby field stars. Contamination is larger to the east ( $\sim 18\%$ ) compared to the west ( $\sim 12\%$ ), which is also as expected. The fitted  $L_3$  for the  $V$ -band light curve of Khaliullin (1985) is formally below 0.2% and not significantly different from zero. Therefore, we find no evidence for the  $\Delta V \approx 1.2$  mag companion reported in the *Tycho* Double Star Catalogue, which if real should contribute about 25% of the light in  $V$ . This star would be expected to be even more prominent in the redder KELT passband, and yet the corresponding  $L_3$  values are smaller than 25%. The radial-velocity offsets  $\Delta$  between the primary and secondary for both RV data sets are also not statistically significant. Repeating the fit with  $L_3(V)$  and the velocity offsets set to zero leads to nearly identical values for all elements. Nevertheless, we have chosen here to retain the results that include these extra parameters, to be conservative, so that any uncertainty in their determination is propagated through to the rest of the adjusted quantities.

The linear limb-darkening coefficient for the  $V$  band,  $0.339^{+0.063}_{-0.032}$ , is somewhat lower than the value of  $\sim 0.45$  expected from theory for the mean temperature of the components (e.g., Claret & Bloemen 2011). The coefficient obtained for the KELT light curves,  $0.408^{+0.077}_{-0.153}$ , is close to the value of 0.38 predicted for the  $R$  band but this is likely accidental as the passbands are not exactly the same.

A graphical representation of the photometric observations and the fitted light curves are given in Figure 2 for the  $V$ -band data of Khaliullin (1985), and in Figure 3 and Figure 4 for the KELT measurements. In each case the residuals are shown below each panel. The resulting scatter of the photometric measurements is 0.015 mag in  $V$ , 0.025 mag for KELT east, and 0.017 mag for KELT west. The CfA RV observations along with those of Lacy (1998) are shown with the fitted model in Figure 5. For the CfA data (71 measurements) the RMS residuals from the fit are 1.51 km s $^{-1}$  and 1.63 km s $^{-1}$  for the primary and secondary, respectively. The 16 measurements by Lacy (1998) show a scatter of 3.54 km s $^{-1}$  and 4.10 km s $^{-1}$ .

## 6. ABSOLUTE DIMENSIONS

The absolute masses and radii of V541 Cyg are listed in Table 6<sup>12</sup>. The relative uncertainties are smaller than 1% in both properties and represent a significant improvement over those obtained by Lacy (1998). Our temperature estimates from Section 2 are marginally different for the two components, and are somewhat higher than those obtained by Guinan et al. (1996),  $T_{\text{eff}} = 9900 \pm 400$  K, and by Lacy (1998),  $T_{\text{eff}} = 9940 \pm 60$  K, both of whom assumed identical temperatures for the two stars.

Strömgren photometry obtained by Lacy (2002) along with the calibration by Crawford (1978) for B-type stars yields a mean reddening of  $E(b - y) = 0.066 \pm 0.005$ , from which  $(b - y)_0 = -0.027 \pm 0.005$  for the combined light. Tabulations by Popper (1980) and Gray (2005) then yield mean temperatures of 10670 K and 10920 K, respectively. Alternatively, the corresponding reddening in the Johnson system,  $E(B - V) = 0.089 \pm 0.007$ , together with the measured  $B - V$  index of Lacy (1992) give  $(B - V)_0 = -0.054 \pm 0.010$ , from which we obtain

<sup>12</sup> The physical constants used in this work conform to IAU Recommendation B3 (Prša et al. 2016).

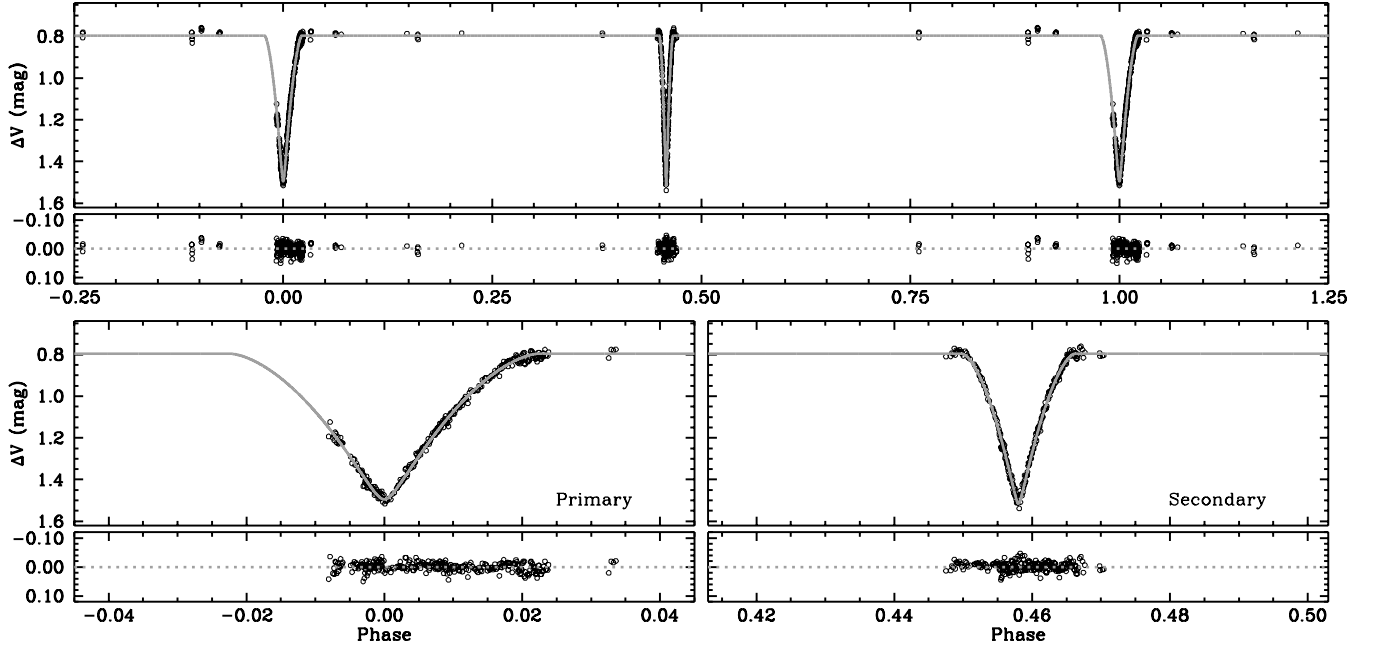


FIG. 2.— Photometry from Khaliullin (1985) in the  $V$  band along with our model light curve, reduced to the reference epoch  $T_0$  in Table 5. Enlargements of the primary and secondary eclipses in the bottom panels have the same horizontal scale to permit a direct comparison of the widths of the eclipses. Residuals from the fit are shown in each panel.

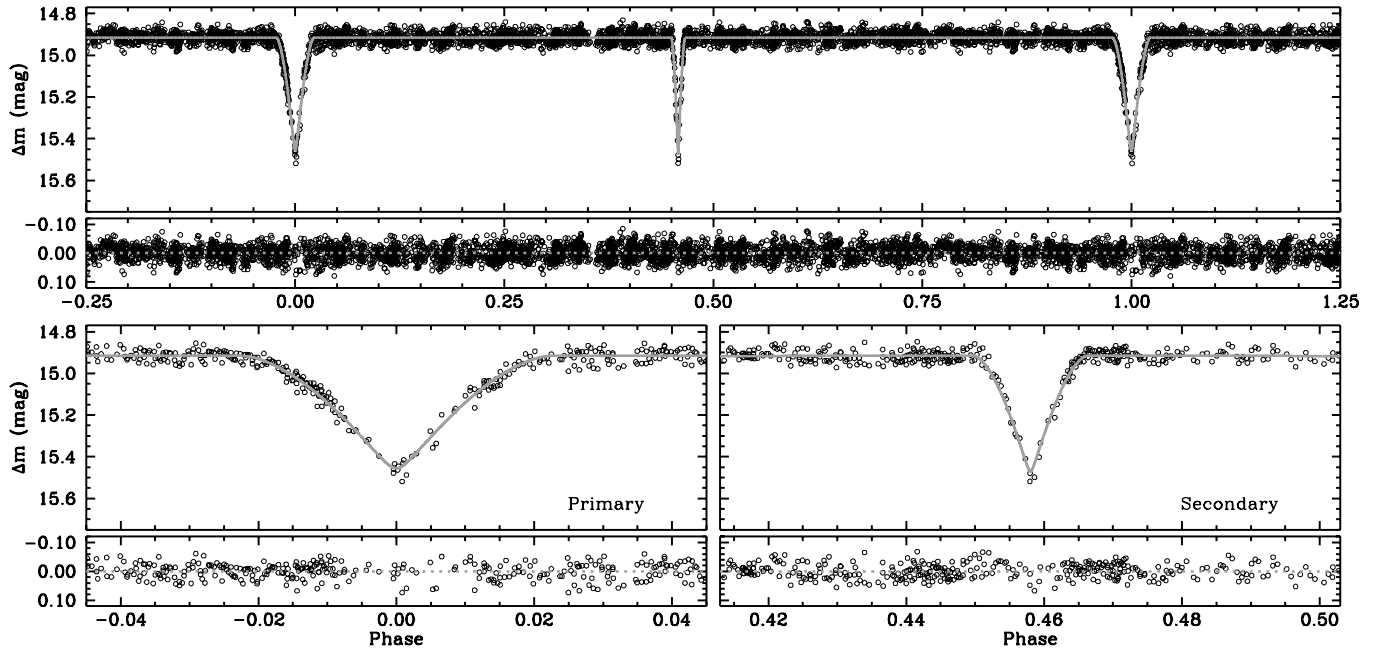


FIG. 3.— Same as Figure 2 for the KELT east photometry.

mean temperatures of 10250 K (Popper 1980), 10890 K (Gray 2005), and 10460 K (Pecaut & Mamajek 2013). The average of the above five photometric estimates,  $10640 \pm 150$  K, is consistent with our spectroscopic determinations ( $10650$  K for the primary and  $10350$  K for the secondary), supporting their accuracy. No spectroscopic metallicity is available for V541 Cyg; our own spectra are unsuitable for a detailed analysis because of the narrow wavelength range, the relatively low signal-to-noise ratios, and the degeneracy with temperature mentioned earlier.

Table 6 lists our measured projected rotational veloc-

ities for the components, which are considerably smaller than earlier estimates of  $20 \pm 5$  km s $^{-1}$  by Guinan et al. (1996) and  $24 \pm 2$  km s $^{-1}$  by Lacy (1998). Also listed are the expected rotational velocities assuming either pseudo-synchronous rotation (Hut 1981) or that the stars are synchronized to the mean orbital motion. The measurements agree well with the pseudo-synchronous values.

## 7. COMPARISON WITH STELLAR EVOLUTION MODELS

The accurate properties derived for V541 Cyg permit an interesting comparison with predictions from cur-

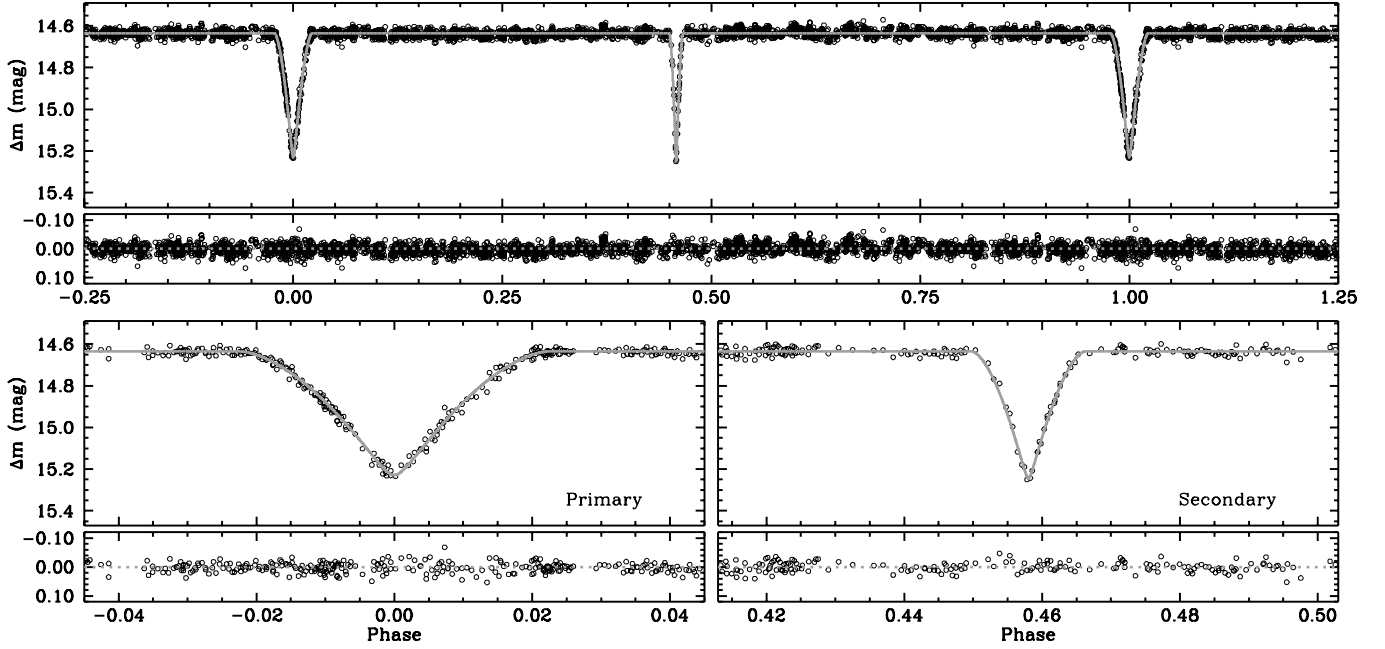


FIG. 4.— Same as Figure 2 for the KELT west photometry.

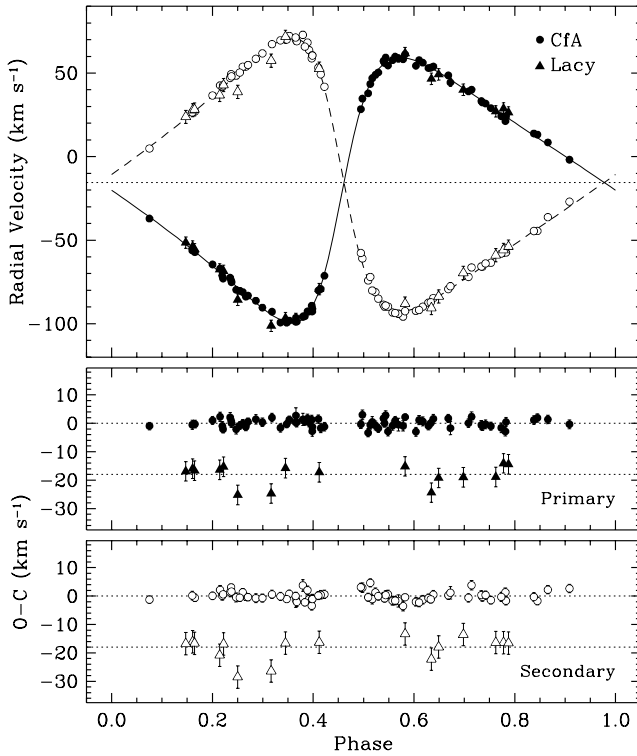


FIG. 5.— Radial-velocity observations of V541 Cyg and orbital fit. Phase 0.0 corresponds to the time of primary eclipse, and the dotted line is the center-of-mass velocity on the CfA reference frame. Measurements for the primary are shown with filled symbols. The observations by Lacy (1998) have been shifted to the CfA frame for display purposes.

rent stellar evolution theory. Figure 6 shows these determinations in the  $\log g$  versus  $T_{\text{eff}}$  plane along with evolutionary tracks for the measured masses from the MESA Isochrones and Stellar Tracks series (MIST; Choi et al. 2016) series, which is based on the Modules for Experiments in Stellar Astrophysics package (MESA; Paxton et al. 2011, 2013, 2015). The metallicity in the

TABLE 6  
PHYSICAL PROPERTIES OF V541 CYG.

| Parameter                                       | Primary                      | Secondary                    |
|---|------------------------------|------------------------------|
| Mass ( $M_{\odot}$ )                            | $2.335^{+0.017}_{-0.013}$    | $2.260^{+0.016}_{-0.013}$    |
| Radius ( $R_{\odot}$ )                          | $1.859^{+0.012}_{-0.009}$    | $1.808^{+0.015}_{-0.013}$    |
| $\log g$ (cgs)                                  | $4.2675^{+0.0052}_{-0.0050}$ | $4.2770^{+0.0072}_{-0.0056}$ |
| Temperature (K)                                 | $10650 \pm 200$              | $10350 \pm 200$              |
| $L/L_{\odot}$                                   | $39.9^{+3.3}_{-2.8}$         | $33.7^{+2.9}_{-2.5}$         |
| $BC_V$ (mag) <sup>a</sup>                       | $-0.39 \pm 0.11$             | $-0.32 \pm 0.11$             |
| $M_{\text{bol}}$ (mag) <sup>b</sup>             | $0.721^{+0.086}_{-0.079}$    | $0.906^{+0.089}_{-0.082}$    |
| $M_V$ (mag)                                     | $1.11 \pm 0.14$              | $1.23 \pm 0.14$              |
| $E(B - V)$ (mag)                                | $0.089 \pm 0.007$            |                              |
| $m - M$ (mag)                                   | $9.66 \pm 0.10$              |                              |
| Distance (pc) <sup>c</sup>                      | $854^{+41}_{-38}$            |                              |
| Parallax (mas)                                  | $1.167^{+0.059}_{-0.050}$    |                              |
| $v_{\text{circ}} \sin i$ (km s <sup>-1</sup> )  | $6.132^{+0.040}_{-0.031}$    | $5.964^{+0.048}_{-0.042}$    |
| $v_{\text{psync}} \sin i$ (km s <sup>-1</sup> ) | $15.50^{+0.11}_{-0.13}$      | $15.09^{+0.09}_{-0.14}$      |
| $v \sin i$ (km s <sup>-1</sup> ) <sup>d</sup>   | $15 \pm 1$                   | $15 \pm 1$                   |

<sup>a</sup> Bolometric corrections from Flower (1996), with a contribution of 0.10 mag added in quadrature to the uncertainty from the temperatures.

<sup>b</sup> Uses  $M_{\text{bol}}^{\odot} = 4.732$  for consistency with the adopted table of bolometric corrections (see Torres 2010).

<sup>c</sup> Relies on the luminosities, the apparent magnitude of V541 Cyg out of eclipse ( $V = 10.350 \pm 0.008$ ; Lacy 1992), and bolometric corrections.

<sup>d</sup> Measured value.

models has been set to  $[\text{Fe}/\text{H}] = -0.18$  in order to match the observations. The models are in excellent agreement with the observations at an age of 190 Myr; an isochrone for this age is shown in the figure with a dashed line. In particular, the temperature difference between the components determined from spectroscopy is consistent with the separation between the evolutionary tracks, which depends on the mass ratio. The stars are seen to be little evolved from the zero-age main sequence. The same comparison is shown in the mass-radius and mass-



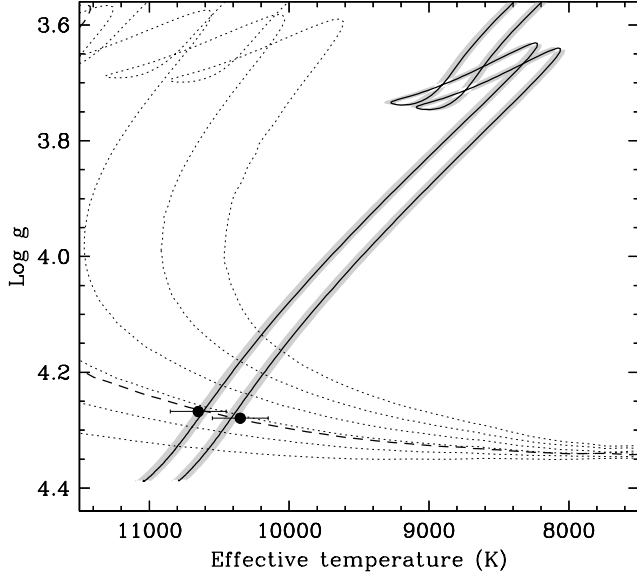


FIG. 6.— Measurements for V541 Cyg in the  $\log g$  vs.  $T_{\text{eff}}$  diagram compared with evolutionary tracks from the MIST series (Choi et al. 2016) for a metallicity of  $[\text{Fe}/\text{H}] = -0.18$  that best matches the observations. The shaded areas around the solid primary and secondary tracks represent the uncertainty in the measured masses. Isochrones ranging from 100 to 350 Myr are shown with dotted lines in steps of 50 Myr, with the best fit at 190 Myr indicated with a heavy dashed line.

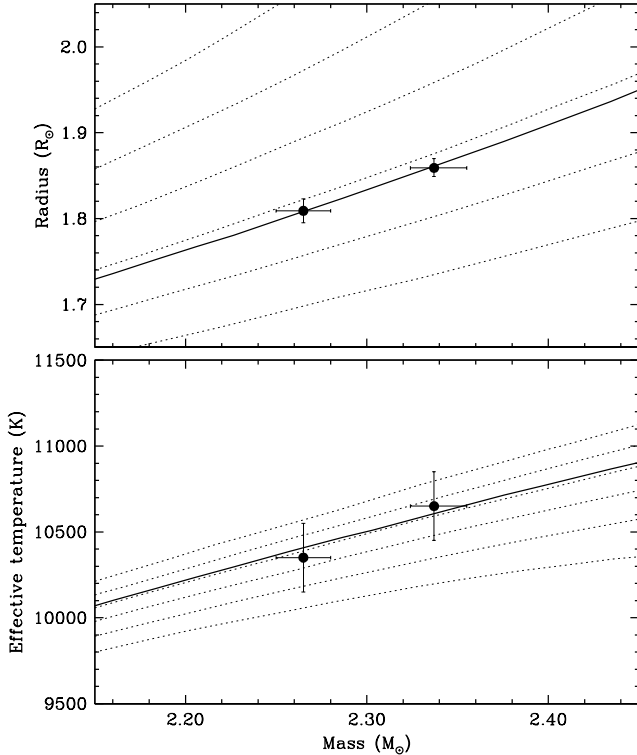


FIG. 7.— Measured masses, radii, and temperatures of V541 Cyg compared against model isochrones from the MIST series (Choi et al. 2016) for the same metallicity of  $[\text{Fe}/\text{H}] = -0.18$  as in Figure 6. Dotted lines represent ages of 100–350 Myr in steps of 50 Myr, and the solid line is the best-fit age of 190 Myr.

temperature diagrams of Figure 7, also indicating good agreement.

## 8. APSIDAL MOTION

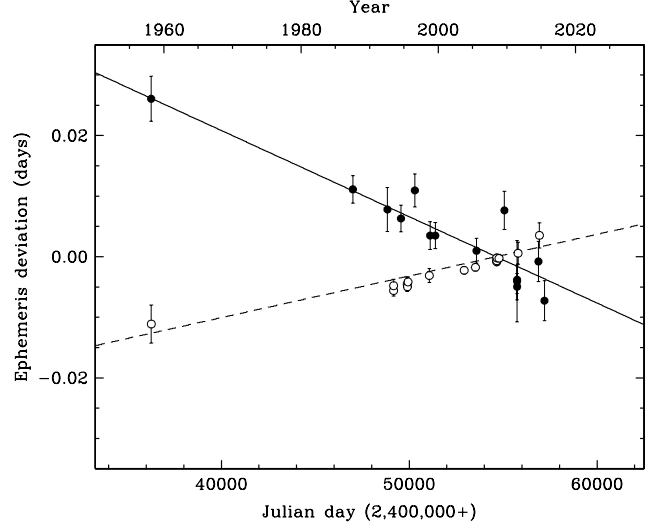


FIG. 8.— Measured times of minimum light from Table 4, and the ephemeris curve from our global fit. Filled circles correspond to primary timings..

Estimates of the rate of apsidal motion for V541 Cyg have varied considerably over the years, beginning with the first measurement by (Khaliullin 1983) yielding  $\dot{\omega} = 1.04 \pm 0.15$  deg century $^{-1}$ , later revised to  $0.90 \pm 0.13$  deg century $^{-1}$  (Khaliullin 1985). A similar estimate of  $0.95 \pm 0.06$  deg century $^{-1}$  was published by Lines et al. (1989). All three studies judged these values to be consistent with expectations from theory (including classical terms and General Relativity), although the physical parameters of the components necessary to compute the predicted apsidal motion rate were not particularly well known at the time, as no dynamical masses were available. Much smaller values of  $\dot{\omega}$  were reported subsequently by Wolf (1995),  $0.53 \pm 0.11$  deg century $^{-1}$ , Guinan et al. (1996),  $0.52 \pm 0.14$  deg century $^{-1}$ , and Lacy (1998),  $0.60 \pm 0.10$  deg century $^{-1}$ , all of whom concluded that the apsidal motion of V541 Cyg was too slow compared to theory. Finally, Volkov & Khaliullin (1999) and Wolf et al. (2010) reported intermediate values of  $0.86 \pm 0.05$  deg century $^{-1}$  and  $0.76 \pm 0.14$  deg century $^{-1}$ , respectively, and considered these to be in good agreement with theory.

The value resulting from our global fit (Table 5),  $\dot{\omega} = 0.859^{+0.042}_{-0.017}$  deg century $^{-1}$ , is more in line with the recent studies and is considerably more precise. It corresponds to an apsidal period of  $U = 41800^{+1000}_{-1800}$  years. The measurements and the computed ephemeris curve are shown in Figure 8.

With the accurate knowledge we now have of the physical properties of the components, we estimate the predicted rate of periastron advance from classical terms (tidal and rotational distortions) to be  $\dot{\omega}_{\text{clas}} = 0.0988^{+0.0062}_{-0.0054}$  deg century $^{-1}$ , where we have adopted identical internal structure constants for the two stars of  $\log k_2 = -2.33 \pm 0.03$  from the models by Claret (2004), for the average mass and age of the system. The general relativistic contribution (e.g., Levi-Civita 1937; Giménez 1985) is calculated to be  $\dot{\omega}_{\text{GR}} = 0.7447^{+0.0032}_{-0.0031}$  deg century $^{-1}$ , which is 7.5 times larger than the classical effect. The total expected apsi-

dal motion is then  $\dot{\omega}_{\text{tot}} = 0.8435^{+0.0073}_{-0.0065}$  deg century $^{-1}$ . This agrees with our measurement within the uncertainties (at the  $0.8\sigma$  level).

## 9. DISCUSSION AND FINAL REMARKS

Our measurements of the properties of V541 Cyg represent an improvement in the precision of the masses of a factor of  $\sim 5$  over the work of Lacy (1998), and a factor of  $\sim 3$  in the radii. Much of this is due to the greater number and higher resolution of our spectroscopic observations, and partly also to the additional light curves from KELT. The absolute dimensions of the system now rank among the best for eclipsing binaries (see, e.g., Torres et al. 2010).

The agreement with stellar evolution theory is excellent, and suggests an age of 190 Myr according to the MIST models. The abundance we infer from this comparison,  $[\text{Fe}/\text{H}] = -0.18$ , is not out of the ordinary. The  $UVW$  space motion components based on our center-of-mass velocity (CfA zero point), distance, and the proper motion from the first data release (DR1) of the *Gaia* mission (Lindegren et al. 2016) are  $U = +1.6$  km s $^{-1}$ ,  $V = -6.8$  km s $^{-1}$ , and  $W = -9.3$  km s $^{-1}$  in the LSR frame.<sup>13</sup> These are typical of the thin disk, as expected from the youth of the system.

V541 Cyg is a member of a very small group of eclipsing systems with well determined properties and accurately measured apsidal motion in which the contribution from General Relativity is significant. In this particular example the GR effect represents 88% of the total predicted motion. Estimates of  $\dot{\omega}$  over the last 30 years have relied almost exclusively on measurements of times of minimum light, and have varied by nearly a factor of two depending largely on the sample of timings used. In addition to having an updated list of historical timings going back to 1958, in this work we have added to the analysis radial velocities spanning 22 years and light curves separated in time by about 30 years, all of which provide additional information constraining the rate of periastron advance. As a result, the formal uncertainty of  $\dot{\omega}$  has been reduced significantly to better than 5%. We find that the observed rate agrees with the predicted rate within the errors, consistent with some of the more recent but less precise estimates from the last 15 years. Even so, it would be of considerable interest to attempt a determination of the orientation of the spin axes of the V541 Cyg components through the Rossiter-McLaughlin effect, which was used successfully in DI Her to show

that the axes of those stars are tilted relative to the orbit, explaining the anomalously slow apsidal motion of that system that had puzzled astronomers for decades. Since there does not appear to be any disagreement with the expected value of  $\dot{\omega}$  for V541 Cyg, we would not expect the spin axes to be strongly misaligned.

Our accurate distance estimate for V541 Cyg leads to an inferred parallax of  $1.167^{+0.059}_{-0.050}$  mas that is marginally consistent with the trigonometric value of  $0.70 \pm 0.34$  mas from the first data release (DR1) of the *Gaia* mission, where the uncertainty quoted in the last value does not include an estimated contribution of 0.30 mas from systematic errors (Lindegren et al. 2016). Recent studies (Stassun & Torres 2016; Jao et al. 2016) have indicated there may in fact be a small but significant bias in the *Gaia* parallaxes of about 0.25 mas, in the sense that the original *Gaia* values are too small. We note that this happens to go in the direction of bringing agreement in the case of V541 Cyg.

Finally, a detailed abundance analysis of V541 Cyg would be highly beneficial as it would permit a more stringent comparison with stellar evolution models than performed here. Because a change in abundance shifts the evolutionary tracks horizontally in Figure 6, knowing the metallicity could serve to test the accuracy of the temperature estimates from this work.

We are grateful to P. Berlind, M. Calkins, R. J. Davis, D. W. Latham, and R. P. Stefanik for help in obtaining the spectroscopic observations of V541 Cyg, and to R. J. Davis and J. Mink for maintaining the CfA echelle database over the years. We also thank J. Irwin for helpful discussions about the use of his light-curve code and for implementing the apsidal motion capability at our request, A. Claret for providing the stellar evolution tracks used for the apsidal motion calculation, and the anonymous referee for a helpful comment. G.T. acknowledges partial support for this work from NSF grant AST-1509375. The efforts of C.M. were supported by the SAO REU program, funded in part by the National Science Foundation REU and Department of Defense AS-SURE programs under NSF Grant No. 1262851, and by the Smithsonian Institution. Work performed by J.E.R. was supported by the Harvard Future Faculty Leaders Postdoctoral fellowship. This research has made use of the SIMBAD and VizieR databases, operated at CDS, Strasbourg, France, and of NASA's Astrophysics Data System Abstract Service.

## REFERENCES

- Agerer, F. 1994, BAV Mitteilungen, No. 68, 5  
 Albrecht, S., Reffert, S., Snellen, I. A. G., & Winn, J. N. 2009, *Nature*, 461, 373  
 Andersen, J., Clausen, J. V., Nordström, B., Tomkin, J., & Mayor, M. 1991, *A&A*, 246, 99  
 Binnendijk, L. 1960, *Properties of Double Stars*, (Philadelphia: Univ. of Pennsylvania Press), p. 308  
 Brát, L., Šmelcer, L., Kuèáková, H., et al. 2008, *Open European Journal on Variable Stars*, 94, 1  
 Choi, J., Dotter, A., Conroy, C., et al. 2016, *ApJ*, 823, 102  
 Claret, A. 1998, *A&AS*, 131, 395  
 Claret, A. 2004, *A&A*, 424, 919  
 Claret, A., & Bloemen, S. 2011, *A&A*, 529, A75  
 Company, R., Portilla, M., & Gimenez, A. 1988, *ApJ*, 335, 962  
 Crawford, D. L. 1978, *AJ*, 83, 48  
 Diethelm, R. 1992a, *BBSAG Bull.*, 99, 10  
 Diethelm, R. 1992b, *BBSAG Bull.*, 102, 4  
 Diethelm, R. 1995, *BBSAG Bull.*, 110, 7  
 Diethelm, R. 1996, *BBSAG Bull.*, 112, 6  
 Diethelm, R. 1999, *BBSAG Bull.*, 120, 4  
 Etzel, P. B. 1980, *EBOP User's Guide*, 3rd. Ed., Dept. of Astron. Univ. California, Los Angeles  
 Etzel, P. B. 1981, *Photometric and Spectroscopic Binary Systems*, Proc. NATO Adv. Study Inst., ed. E. B. Carling & Z. Kopal (Dordrecht: Reidel), p. 111  
 Fabricius, C., Høg, E., Makarov, V. V., et al. 2002, *A&A*, 384, 180  
 Flower, P. J. 1996, *ApJ*, 469, 355

<sup>13</sup>  $U$  is counted positive toward the Galactic center.

- Foreman-Mackey, D., Hogg, D. W., Lang, D., & Goodman, J. 2013, *PASP*, 125, 306
- Giménez, A. 1985, *ApJ*, 297, 405
- Goodman, J., & Weare, J. 2010, *Commun. Appl. Math. Comput. Sci.*, 5, 65
- Gray, D. F. 2005, *The Observation and Analysis of Stellar Photospheres*, 3rd Ed., Cambridge Univ. Press, p. 506
- Gregory, P. C. 2005, *ApJ*, 631, 1198
- Guinan, E. F., & Maloney, F. P. 1985, *AJ*, 90, 1519
- Guinan, E. F., Maley, J. A., & Marshall, J. J. 1996, *Information Bulletin on Variable Stars*, 4362, 1
- Hoňková, K., Juryšek, J., Lehký, M., et al. 2013, *Open European Journal on Variable Stars*, 160, 1
- Hübscher, J., Lehmann, P. B., Monninger, G., Steinbach, H.-M., & Walter, F. 2010, *Information Bulletin on Variable Stars*, 5941, 1
- Hübscher, J., Lehmann, P. B., & Walter, F. 2012, *Information Bulletin on Variable Stars*, 6010, 1
- Hübscher, J., & Lehmann, P. B. 2012, *Information Bulletin on Variable Stars*, 6026, 1
- Hübscher, J., & Lehmann, P. B. 2015, *Information Bulletin on Variable Stars*, 6149, 1
- Hübscher, J. 2015, *Information Bulletin on Variable Stars*, 6152, 1
- Hübscher, J. 2016, *Information Bulletin on Variable Stars*, 6157, 1
- Hut, P. 1981, *A&A*, 99, 126
- Irwin, J. M., Quinn, S. N., Berta, Z. K., et al. 2011, *ApJ*, 742, 123
- Jao, W.-C., Henry, T. J., Riedel, A. R., Winters, J. G., Slatten, K. J., & Gies, D. R., *ApJ*, in press (arXiv:1611.00656)
- Karpowicz, M. 1961, *Acta Astron.*, 11, 51
- Khaliullin, K. F. 1983, *Astronomicheskij Tsirkulyar*, 1270, 1
- Khaliullin, K. F. 1985, *ApJ*, 299, 668
- Kitamura, M., & Nakamura, Y. 1983, *Annals of the Tokyo Astronomical Observatory*, 19, 413
- Kopal, Z. 1959, *Close Binary Systems*, The International Astrophysics Series, (London: Chapman & Hall), p. 170
- Kuhn, R. B., Rodriguez, J. E., Collins, K. A., et al. 2016, *MNRAS*, 459, 4281
- Kovács, G., Bakos, G., & Noyes, R. W. 2005, *MNRAS*, 356, 557
- Kulikowski, P. G. 1948, *Perem. Zvezdy*, 6, 101
- Kulikowski, P. G. 1953, *Perem. Zvezdy*, 9, 169
- Lacy, C. H. S., Clem, J. L., Zakirov, M., et al. 1998, *Information Bulletin on Variable Stars*, 4597, 1
- Lacy, C. H. S. 1998, *AJ*, 115, 801
- Lacy, C. H. S. 1992, *AJ*, 104, 2213
- Lacy, C. H. S. 2002, *AJ*, 124, 1162
- Latham, D. W. 1992, in *IAU Coll. 135, Complementary Approaches to Double and Multiple Star Research*, ASP Conf. Ser. 32, eds. H. A. McAlister & W. I. Hartkopf (San Francisco: ASP), 110
- Latham, D. W., Nordström, B., Andersen, J., Torres, G., Stefanik, R. P., Thaller, M., & Bester, M. 1996, *A&A*, 314, 864
- Latham, D. W., Stefanik, R. P., Torres, G., Davis, R. J., Mazeh, T., Carney, B. W., Laird, J. B., & Morse, J. A. 2002, *AJ*, 124, 1144
- Levi-Civita, T. 1937, *Am. J. Math.*, 59, 225
- Lindegren, L., Lammers, U., Bastian, U. et al. 2016, *A&A*, in press (arXiv:1609.04303)
- Lines, R. D., Lines, H., Guinan, E. F., & Carroll, S. M. 1989, *Information Bulletin on Variable Stars*, 3286, 1
- Lucy, L. B. 1967, *ZAp*, 65, 89
- Martynov, D. Ya. 1973, *Eclipsing Variable Stars*, ed. V. P. Tsevesich, (Jerusalem: Halsted Press), p. 128
- Mason, B. D., Hartkopf, W. I., Gies, D. R., Henry, T. J., & Helsel, J. W. 2009, *AJ*, 137, 3358
- Nordström, B., Latham, D. W., Morse, J. A., Milone, A. A. E., Kurucz, R. L., Andersen, J., & Stefanik, R. P. 1994, *A&A*, 287, 338
- Paxton, B., Bildsten, L., Dotter, A., et al. 2011, *ApJS*, 192, 3
- Paxton, B., Cantiello, M., Arras, P., et al. 2013, *ApJS*, 208, 4
- Paxton, B., Marchant, P., Schwab, J., et al. 2015, *ApJS*, 220, 15
- Pecaut, M. J., & Mamajek, E. E. 2013, *ApJS*, 208, 9
- Pepper, J., Pogge, R. W., DePoy, D. L., et al. 2007, *PASP*, 119, 923
- Pepper, J., Kuhn, R. B., Siverd, R., James, D., & Stassun, K. 2012, *PASP*, 124, 230
- Popper, D. M. 1980, *ARA&A*, 18, 115
- Popper, D. M., & Etzel, P. B. 1981, *AJ*, 86, 102
- Prša, A., Harmanec, P., Torres, G., et al. 2016, *AJ*, 152, 41
- Sandberg Lacy, C. H., Zakirov, M., Arzumanyants, G., et al. 1995, *Information Bulletin on Variable Stars*, 4194, 1
- Siverd, R. J., Beatty, T. G., Pepper, J., et al. 2012, *ApJ*, 761, 123
- Southworth, J. 2013, *A&A*, 557, A119
- Smith, A. B., & Caton, D. B. 2007, *Information Bulletin on Variable Stars*, 5745, 1
- Stassun, K. G., & Torres, G. 2016, *ApJ*, in press (arXiv:1609.05390)
- Torres, G. 2010, *AJ*, 140, 1158
- Torres, G., Andersen, J., & Giménez, A. 2010, *A&A Rev.*, 18, 67
- Torres, G., Stefanik, R. P., Andersen, J., et al. 1997, *AJ*, 114, 2764
- Torres, G., Neuhäuser, R., & Guenther, E. W. 2002, *AJ*, 123, 1701
- Volkov, I. M., & Khaliullin, K. F. 1999, *Information Bulletin on Variable Stars*, 4680, 1
- von Zeipel, H. 1924, *MNRAS*, 84, 702
- Wolf, M. 1995, *Information Bulletin on Variable Stars*, 4217, 1
- Wolf, M., Claret, A., Kotková, L., et al. 2010, *A&A*, 509, A18
- Zucker, S., & Mazeh, T. 1994, *ApJ*, 420, 806